

## Asymptotic Behavior of the Vertex Function in Quantum Electrodynamics\*

Paul M. Fishbane and J. D. Sullivan

*Physics Department, University of Illinois, Urbana, Illinois 61801*

(Received 11 February 1971)

Using recently developed infinite-momentum techniques, we study the asymptotic behavior of the three-point function in quantum electrodynamics (massive photons) by summing the leading behavior of the perturbation series. We find that the leading diagrams are those in which photons are exchanged in all permutations across the external photon insertion. When the fermion lines are on-shell, we confirm an earlier speculation of Jackiw based on a fourth-order calculation, namely, that the vertex exponentiates in the form  $\bar{u}(p_f)\Lambda^\mu u(p_i) = \bar{u}(p_f)\gamma^\mu u(p_i)e^{-\Phi}$ , where  $\Phi = (e^2/16\pi^2)\ln^2(Q^2/\mu^2)$ . In a fashion which is reminiscent of eikonalization in a scattering process,  $\Phi$  is characteristic of single-photon exchange across the vertex. We also identify and compute an  $O(e^4)$  contribution to  $\Phi$  coming from vacuum polarization. We discuss the concept of infinite-momentum pathways, the possibility of exponentiation in scalar theories, and speculate on extensions of our work.

### I. INTRODUCTION

Considerable progress has recently been made in the calculation of the high-energy asymptotic behavior of scattering amplitudes through summation of the leading terms of infinite sets of perturbation theory diagrams.<sup>1</sup> It is in precisely such asymptotic limits, where the effects of resonances and other local properties should be smoothed out, that one can hope to see general features suggested by field theories. Interest in this worthwhile activity has been heightened by, among other things, the experimental discovery in inelastic electron-proton scattering of an apparent pointlike substructure in the proton and other questions of scaling in high-energy reactions.<sup>2</sup>

So far most work has been devoted to the study of two-particle to two-particle processes and, more recently, two-particle to  $n$ -particle<sup>3</sup> processes. An important breakthrough behind this work has been the development of "infinite-momentum"<sup>4</sup> techniques which allow the extraction of leading asymptotic terms of perturbation-theory diagrams without recourse to the usual Feynman parametrization. We report in this work a calculation for a well-defined gauge-invariant set of diagrams of the asymptotic momentum-transfer behavior of the elastic form factor in spinor-vector field theory [quantum electrodynamics (QED) with massive photons]. We make use of the "infinite-momentum" techniques, appropriately modified, in our work and find that they lead to considerable simplification, as was the case for scattering amplitudes.

The asymptotic behavior of the nucleon form factor in pseudoscalar pion-nucleon field theory, with and without isospin, has been extensively studied in a recent admirable paper by Applequist and Primack.<sup>5</sup> We ignore isospin throughout all

our work and refer the interested reader to Ref. 5 for a demonstration of the extreme difficulties generated by the introduction of isospin, as well as an excellent review of previous attempts to study the asymptotic behavior of three-point functions from various points of view.

The elastic form factor for spinor-vector field theory, the object of this paper, has been partially examined previously. Cassandro and Cini<sup>6</sup> computed the asymptotic behavior of all uncrossed-ladder diagrams, and more recently Jackiw<sup>7</sup> computed in addition the contribution of the lowest, fourth-order crossed-ladder diagram. On the basis of his calculations Jackiw conjectured that the contribution from the sum of all crossed- and uncrossed-ladder diagrams would exponentiate in the form

$$\begin{aligned} \bar{u}(p_b)\Lambda^\mu(Q^2, p_b^2 = m^2, p_a^2 = m^2)u(p_a) \\ = \bar{u}(p_b)\gamma^\mu u(p_a)\exp\left(-\frac{e^2}{16\pi^2}\ln^2(Q^2/\mu^2)\right), \end{aligned}$$

where  $Q^2$  is the asymptotically large momentum transfer. (See Sec. II for the definition of other quantities in this equation.)

The major contribution we are reporting here is a proof that this conjecture is indeed true to all orders, and that nonladder contributions are not as asymptotically large. With no extra work we are also able to calculate and show the exponentiation of the form factor for off-shell fermions  $p_a^2 \neq m^2$ ,  $p_b^2 \neq m^2$ , and in the far-off-shell limit  $Q^2 \gg |p_a^2|$ ,  $|p_b^2| \gg m^2$  we recover the result obtained long ago by Sudakov.<sup>8</sup> So far not included are photon-photon scattering insertions. We also discuss the cases of scalar-vector field theory (Appendix B) as well as a theory with only scalar fields.

An outline of our paper is as follows. In Sec. II we present the relevant kinematics and notation. In Sec. III we study in some detail low-order diagrams for this process. The purpose of Sec. III is to give the reader some feel for the approximations involved and as to why the infinite-momentum-variable approach is a particularly simple one to use. We also identify which types of diagrams give the leading behavior and which types contribute only to nonleading terms. In Sec. IV we study the more general case. We show how the sum over multiple-photon exchange, which contributes the leading terms in any order, leads to a falling exponential whose argument depends only on single-photon exchange. In Sec. V we show how the results of the previous section can and cannot be applied to simple three-point scalar theories. The discussion of Sec. V revolves around the simple identification of infinite-momentum pathways. We find problems similar to those which have been found in the study of scattering in scalar theories, namely "shortcuts" for infinite momentum which wreck the simple exponentiation of leading terms.

In Sec. VI we present our conclusions and some speculations.

In Appendix A we study a certain key integral which arises in all orders. In Appendix B we examine the (trivial) modifications in the scalar-vector theory.

## II. KINEMATICS AND NOTATION

The object of our study is the vertex  $\Lambda^\mu(q^2, p_b^2, p_a^2)$  which describes the absorption of a virtual photon of 4-momentum  $q$  by a fermion of 4-momentum  $p_a$ , resulting in a final fermion of 4-momentum  $p_b = p_a + q$ . [See Fig. 1(a).] We carry out all calculations for values of  $q^2$ , the squared momentum transfer, which are spacelike ( $q^2 < 0$ ) and large in magnitude compared to *all* other parameters (masses) in the problem. Our experience with calculations for lowest-order diagrams in the large timelike region of  $q^2$  indicates that the dispersive (real) part of the vertex is always at least one power of  $\ln|q^2|$  larger than the absorptive (imaginary) part. Thus we believe that our answer for large spacelike values may be freely continued to the large timelike region and remains valid.

The object of greatest physical interest is the vertex with both fermions on shell, namely  $p_a^2 = p_b^2 = m^2$ . However, it is useful and no more work to simultaneously handle the off-mass-shell case and we do so. For technical convenience we will suppose that when  $p_a^2$  and  $p_b^2$  are off shell it is in the spacelike direction, namely,

$$p_a^2 \equiv m_a^2 \leq m^2, \quad p_b^2 \equiv m_b^2 \leq m^2.$$

Since  $q^2$  is spacelike, we are free to go to a (Breit) frame where  $q^0 = 0$ . We denote the space part of  $q$  in such a frame by  $Q^i$  and suppose it to lie along the  $+z$  direction. Thus  $-q_\mu q^\mu = Q^i Q^i \equiv Q^2$  will always denote a positive quantity. There is no loss of generality in further assuming that the space parts of  $p_a$  and  $p_b$  have only  $z$  components as drawn in Fig. 1(b). As  $Q^2 \rightarrow \infty$ , particle  $a$  is moving rapidly in the  $-z$  direction and  $b$  is moving rapidly in the  $+z$  direction. In view of this it is natural, therefore, to use the so-called "infinite-momentum" variables<sup>4</sup> which are a simple rotation of the usual space-time components of 4-vectors. Instead of denoting a 4-vector  $a^\mu$  by  $(a^0, a^1, a^2, a^3)$  we denote it by  $(a^+, \vec{a}, a^-)$ , where  $a^\pm = a^0 \pm a^3$  and  $\vec{a} = (a^1, a^2)$  denotes a 2-vector in the  $xy$  plane. In terms of these variables  $a \cdot b = \frac{1}{2}(a^+ b^- + a^- b^+) - \vec{a} \cdot \vec{b}$ ; in particular the mass shell condition is  $a^2 = a^+ a^- - \vec{a}^2$ .

These variables are useful because particle  $a$ , moving rapidly (for  $Q^2 \rightarrow \infty$ ) in the negative  $z$  direction, has a large  $p_a^-$  and a small,  $O(1/p_a^-)$ ,  $p_a^+$  component. Conversely, particle  $b$ , moving rapidly in the positive  $z$  direction, has a large  $p_b^+$  and a small  $p_b^-$ .

Thus for  $Q^2 \rightarrow \infty$  we have in this special frame

$$\begin{aligned} q^\mu &= (Q, \vec{0}, -Q), \\ p_a^\mu &= (m_a^2/Q, \vec{0}, Q) + O(1/Q^3, \vec{0}, 1/Q), \\ p_b^\mu &= (Q, \vec{0}, m_b^2/Q) + O(1/Q, \vec{0}, 1/Q^3), \end{aligned} \quad (2.1)$$

where  $Q^2 \gg |m_a^2|, |m_b^2|$  and  $Q > 0$ .

Finally, we briefly recall the well-known description of the elastic form factors. The on-shell vertex has the form

$$\begin{aligned} \bar{u}(p_b) \Lambda^\mu(q^2, m^2, m^2) u(p_a) \\ = \bar{u}(p_b) [F_1(q^2) \gamma^\mu + i \sigma^{\mu\nu} q^\nu F_2(q^2)] u(p_a). \end{aligned} \quad (2.2)$$

When we calculate below the leading contribution to Eq. (2.2) in each order of perturbation theory

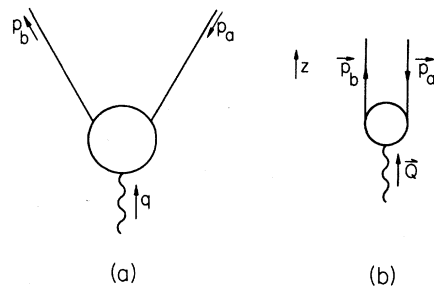


FIG. 1. (a) The three-point process we study.  $q$  is spacelike. (b) A convenient coordinate system puts all three particles collinear along the  $z$  axis.

we find a result proportional to  $\bar{u}\gamma^\perp u$ , where  $\gamma^\perp$  stands for  $\gamma^x$  or  $\gamma^y$ . This indicates that, at least for the diagrams we consider,  $F_2(q^2)/F_1(q^2) = O(1/Q^2)$  as  $Q^2 \rightarrow \infty$ . This is not a surprising result and is in accord with experiment as well as other theoretical considerations. Physically it corresponds to the conservation of the fermion's helicity. Except that  $F_2$  is asymptotically smaller than  $F_1$ , we learn nothing from our work about  $F_2$ .

For the off-shell vertex, the spinors in Eq. (2.2) are replaced by projection operators and a more general decomposition involving twelve form factors holds. If we introduce

$$\Lambda_\pm(p) = (2m)^{-1}(m \pm \not{p}), \quad (2.3)$$

then the general structure of the fully off-shell vertex may be written

$$\begin{aligned} \Lambda^\mu(q^2, p_b^2, p_a^2) = & \Lambda_+(p_b)(\mathcal{F}_1\gamma^\mu + i\mathcal{F}_2\sigma^{\mu\nu}q^\nu + \mathcal{F}_3q^\mu)\Lambda_+(p_a) \\ & + \Lambda_-(p_b)(\mathcal{F}_4\gamma^\mu + i\mathcal{F}_5\sigma^{\mu\nu}q^\nu + \mathcal{F}_6q^\mu)\Lambda_-(p_a) \\ & + \Lambda_+(p_b)(\mathcal{F}_7\gamma^\mu + i\mathcal{F}_8\sigma^{\mu\nu}q^\nu + \mathcal{F}_9q^\mu)\Lambda_-(p_a) \\ & + \Lambda_-(p_b)(\mathcal{F}_{10}\gamma^\mu + i\mathcal{F}_{11}\sigma^{\mu\nu}q^\nu + \mathcal{F}_{12}q^\mu)\Lambda_+(p_a). \end{aligned} \quad (2.4)$$

In Eq. (2.4) each of the twelve form factors is a function of the three scalar variables  $q^2$ ,  $p_a^2 = m_a^2$ ,  $p_b^2 = m_b^2$ . On shell, only  $\mathcal{F}_{1,2,3}$  are coupled and  $\mathcal{F}_{1,2}(q^2, m^2, m^2) = F_{1,2}(q^2)$ ,  $\mathcal{F}_3(q^2, m^2, m^2) = 0$ .<sup>9</sup>

Charge-conjugation invariance implies

$$C\Lambda_\mu^T(-p_a, -p_b)C^{-1} = -\Lambda_\mu(p_b, p_a), \quad (2.5)$$

where  $C$  is the usual charge-conjugation matrix satisfying  $C^T = -C$  and  $C\gamma^\mu C^{-1} = -\gamma^\mu$ . Equation (2.5) yields the following conditions on the twelve form factors:

$$\begin{aligned} \mathcal{F}_i(q^2, p_b^2, p_a^2) &= \mathcal{F}_i(q^2, p_a^2, p_b^2), & i = 1, 2, 4, 5 \\ \mathcal{F}_j(q^2, p_b^2, p_a^2) &= -\mathcal{F}_j(q^2, p_a^2, p_b^2), & j = 3, 6 \\ \mathcal{F}_k(q^2, p_b^2, p_a^2) &= \mathcal{F}_{k+3}(q^2, p_a^2, p_b^2), & k = 7, 8 \\ \mathcal{F}_9(q^2, p_b^2, p_a^2) &= -\mathcal{F}_{12}(q^2, p_a^2, p_b^2). \end{aligned} \quad (2.6)$$

We will see that our calculations give, up to powers of  $\ln Q^2$ ,  $\Lambda^\mu(q^2, p_b^2, p_a^2) \sim \gamma^\perp \gamma^\perp \gamma^\perp$ .

This implies that for  $Q^2 \gg |m_a^2|, |m_b^2|$ , only the charge-type form factors are large, namely,

$$\mathcal{F}_i(Q^2, m_b^2, m_a^2) = \mathcal{F}_i(Q^2, m_b^2, m_a^2) + O(1/Q^2),$$

$$i = 4, 7, 10$$

and

$$\mathcal{F}_j(Q^2, m_b^2, m_a^2)/\mathcal{F}_i(Q^2, m_b^2, m_a^2) = O(1/Q^2),$$

$$j = 2, 3, 5, 6, 8, 9, 11, 12$$

as  $Q^2 \rightarrow \infty$ . Thus equipped, we now turn to the calculation of the three-point function.

### III. LOW-ORDER CALCULATIONS

We examine in this section the asymptotic behavior of the second- and fourth-order diagrams which contribute to the vertex. Special attention is paid to what approximations can and cannot be made in the integrand before the loop integrations are performed. We show which diagrams contribute most strongly as  $Q^2 \rightarrow \infty$  and calculate the precise contributions of these diagrams. The insight obtained from these lower-order calculations will enable us to generalize our results to all orders in Sec. IV.

#### A. Calculation of Order $e^2$

The only diagrams which contribute to this order are shown in Fig. 2. Let us first consider Fig. 2(a) and initially neglect the numerator of the Feynman integral which arises from the spins of the fermions and the photon. One has

$$\begin{aligned} \Gamma^{(1)} = & ie^2 \int \frac{d^4k}{(2\pi)^4} [(p_a + k)^2 - m^2 + i\epsilon]^{-1} \\ & \times [(p_b + k)^2 - m^2 + i\epsilon]^{-1} (k^2 - \mu^2 + i\epsilon)^{-1}, \end{aligned} \quad (3.1)$$

where we have given the photon a mass  $\mu$  to avoid uninteresting infrared difficulties. We may approximate the fermion propagators by

$$(p_a + k)^2 - m^2 + i\epsilon = k^+(Q + k^-) - a + i\epsilon + O(1/Q), \quad (3.2)$$

$$(p_b + k)^2 - m^2 + i\epsilon = k^-(Q + k^+) - b + i\epsilon + O(1/Q),$$

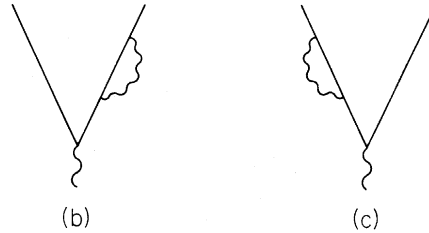
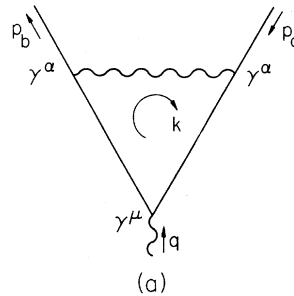


FIG. 2. The three diagrams of second order. (b) and (c) merely generate mass and wave-function renormalization.

and write the photon propagator (no approximation)

$$k^2 - \mu^2 + i\epsilon = k^+ k^- - \Delta + i\epsilon, \quad (3.3)$$

where for convenience we have introduced

$$\begin{aligned} a &= \vec{k}^2 + m^2 - m_a^2, \\ b &= \vec{k}^2 + m^2 - m_b^2, \\ \Delta &= \vec{k}^2 + \mu^2. \end{aligned} \quad (3.4)$$

Using  $d^4k = \frac{1}{2} d^2k dk^- dk^+$ , we cast Eq. (3.1) into the form

$$\begin{aligned} \Gamma^{(1)} &= \frac{ie^2}{2(2\pi)^4} \int d^2k \int_{-\infty}^{+\infty} dk^- \int_{-\infty}^{+\infty} dk^+ [k^+(Q+k^-) - a + i\epsilon]^{-1} \\ &\quad \times [k^-(Q+k^+) - b + i\epsilon]^{-1} (k^+ k^- - \Delta + i\epsilon)^{-1}. \end{aligned} \quad (3.5)$$

All integrations in Eq. (3.5) are convergent, so the neglect of the  $O(1/Q)$  corrections in Eq. (3.2) which we have made in writing Eq. (3.5) is fully justified.

The most gross approximation would be to further neglect the  $O(Q^0)$  terms in Eq. (3.2), i.e., to simplify the first two factors in the integrand according to  $[k^+(Q+k^-) - a][k^-(Q+k^+) - b] \rightarrow Q^2 k^+ k^-$ . We would have then logarithmic divergences coming from the regions of *small*  $k^+$ , *small*  $k^-$ , and *large*  $\vec{k}^2$  suggesting

$$\Gamma^{(1)} = -\frac{e^2}{2(2\pi)^3} \frac{1}{Q^2} \int d^2k \int_{-Q}^0 dk^- \left(1 + \frac{k^-}{Q}\right) \left[ k^- \left(1 + \frac{k^-}{Q}\right) - \frac{b}{Q} + \frac{k^-(a-b)}{Q^2} \right]^{-1} \left[ \Delta \left(1 + \frac{k^-}{Q}\right) - \frac{k^-}{Q} a \right]^{-1}. \quad (3.6)$$

If we take the limit  $Q \rightarrow \infty$  in this integrand, we see the logarithmic divergences at small  $k^-$  and large  $\vec{k}^2$  anticipated above. To extract the precise asymptotic form we note first that the  $O(1/Q^2)$  term in the integrand can be dropped without losing convergence, but not *all* the  $O(1/Q)$  terms. In the vicinity of the lower limit,  $(1+k^-/Q) < \epsilon \ll 1$ , the numerator vanishes, making it impossible to build up a  $\ln Q^2$  enhancement. More strongly, in the entire region  $0 \leq (1+k^-/Q) < 1 - \epsilon'$ ,  $\epsilon' \ll 1$ , no logarithmic buildup is possible since the first denominator factor in the integrand is behaving as  $(k^-)^2$ . Thus we may make the replacement  $(1+k^-/Q) \rightarrow 1$  everywhere in Eq. (3.6) without affecting the asymptotic behavior. This leads to the form

$$\Gamma^{(1)} = \frac{e^2}{2(2\pi)^3} \frac{1}{Q^2} \int d^2k \int_{-\epsilon Q}^0 dk^- \left(k^- - \frac{b}{Q}\right)^{-1} \left(\frac{k^- a}{Q} - \Delta\right)^{-1}. \quad (3.7)$$

The integrand in Eq. (3.7) damps rapidly for  $\vec{k}^2 > Q^2$ , and thus we may cut off the transverse integrations at  $\vec{k}^2 = \lambda Q^2$ ,  $\lambda \ll 1$  in extracting the leading asymptotic behavior.<sup>11</sup> We reserve for Appendix A evaluation of Eq. (3.7), but merely quote here the results in two simple regimes. On shell,  $m_a^2 = m_b^2 = m^2$ , we find [see Eq. (A3)]

$$\Gamma^{(1)} = + \left(\frac{e^2}{16\pi^2}\right) \frac{1}{2Q^2} \ln^2(Q^2/\mu^2) + O(Q^{-2} \ln Q^2). \quad (3.8)$$

For off the mass shell,  $Q^2 \gg |m_a^2|, |m_b^2| \gg m^2$ ,  $|m_a^2 m_b^2| / (Q^2 \mu^2) \gg Q^2$  [see Eq. (A4)],

$$\Gamma^{(1)} \sim (1/Q^2) \ln^3 Q^2.$$

Actually, as we shall see immediately from a more careful treatment, one of the logarithmic factors coming from the small  $k^+$ ,  $k^-$  region cancels because of oddness of the integrand, and the true asymptotic behavior is

$$\Gamma^{(1)} \sim (1/Q^2) \ln^2 Q^2.$$

Except for this cancellation, the insights gained from this most gross approximation are valid and provide a powerful guide in the higher orders. For the sake of discussion we shall refer to the  $\ln Q^2$  coming from the large  $\vec{k}^2 \approx Q^2$  region as an ultraviolet logarithm, and the  $\ln Q^2$  coming from the small  $k^+$ ,  $k^-$  region as an infrared logarithm.<sup>10</sup> Because of the cancellation just mentioned of a potential infrared  $\ln^2 Q^2$ , it is not possible to precisely assign the single infrared  $\ln Q^2$  which does occur to either the small- $k^+$  or small- $k^-$  integration, even though we may sometimes appear to be doing so when we are drawing attention to certain regions of integration.

Return now to Eq. (3.5) and carry out the  $k^+$  integration by contour integration. Examination of the  $i\epsilon$ 's reveals that unless  $k^-$  is restricted to the interval  $-Q < k^- < 0$ , all poles lie in the lower  $k^+$  plane and the integral vanishes identically; hence

$$\Gamma^{(1)} = + \left(\frac{e^2}{8\pi^2}\right) \frac{1}{2Q^2} \ln\left(\frac{Q^2}{m_a^2}\right) \ln\left(\frac{Q^2}{m_b^2}\right) + O(Q^{-2} \ln Q^2). \quad (3.9)$$

The latter limit is the one examined by Sudakov.<sup>8</sup>

Thus we have established the crucial result that the dominant asymptotic behavior comes from regions of integration where all components of  $k$  are less than  $Q$ .<sup>12</sup> In the light of this we may go back to Eq. (3.5) and make the replacements  $Q+k^- \rightarrow Q$ ,  $Q+k^+ \rightarrow Q$ . Doing so, and performing the now simpler  $k^+$  integration by contour inte-

gration, we find immediately without further approximation an equation which differs from (3.7) only in replacement of the lower limit of the  $k^-$  integration by  $-\infty$ . However, the region from  $-\epsilon Q$  to  $-\infty$  cannot contribute a logarithm, so this change is insignificant.

Let us now return to the more physical case of fermions and photons with spin. The integrand in Eq. (3.1) acquires a numerator<sup>13</sup>:

$$N^\mu(Q, k) = -\bar{u}(p_b)\gamma^\alpha(\not{p}_b + \not{k} + m)\gamma^\mu(\not{p}_a + \not{k} + m)\gamma^\alpha u(p_a). \quad (3.10)$$

The presence of the two powers of the loop momentum in  $N$  leads to the well-known ultraviolet divergence of the vertex in QED. We renormalize this divergence by subtracting the integrand from itself at  $Q=0$ ,

$$\Lambda_{(1)}^\mu = ie^2 \int \frac{d^4k}{(2\pi)^4} \left[ \frac{N^\mu(Q, k)}{D(Q, k)} - \frac{N^\mu(0, k)}{D(0, k)} \right], \quad (3.11)$$

where  $D(Q, k)$  stands for the three propagator factors in Eq. (3.1). After this renormalization has been made, and we take the large- $Q^2$  limit, the important range of integration is again  $k$  bounded by  $Q$ , i.e.,  $|k^\nu| < \epsilon Q$ , as in the scalar case. Thus all the previous approximations we made for  $D$  remain valid and, moreover, we may neglect  $k$  in comparison to  $Q$  in evaluating  $N(Q, k)$ . To see this, remove the subtraction term by differentiating Eq. (3.11) once with respect to  $Q$  (prime denotes this differentiation),

$$\Lambda_{(1)}^{\mu'} = ie^2 \int d^4k \left[ N^{\mu'}(Q, k) \frac{1}{D(Q, k)} + N^\mu(Q, k) \left( \frac{1}{D(Q, k)} \right)' \right]. \quad (3.12)$$

Both terms in Eq. (3.12) converge by themselves and have a large- $k$  behavior identical to the scalar case, Eq. (3.1). For the first term this is true because  $N^{\mu'}$  loses one power of  $k$  through the differentiation and loses a second power by symmetry; the second term in the integrand has an additional  $k^2$  factor in the denominator compensating the  $k^2$  growth of  $N^\mu$  at large  $k$ .

Thus we may simplify  $N^\mu$  [Eq. (3.10)] by neglecting  $k$  everywhere compared to  $Q$ , and hence asymptotically

$$\Lambda_{(1)}^{\mu'} = N^{\mu'}(Q \rightarrow \infty)\Gamma^{(1)}(Q) + N^\mu(Q \rightarrow \infty)\Gamma^{(1)'}(Q) = [N^\mu(Q \rightarrow \infty)\Gamma^{(1)}(Q)]'. \quad (3.13)$$

### B. Order- $e^4$ Calculation

The diagrams in  $O(e^4)$  are shown in Fig. 3. Let us first study diagram 3(a) with loop momenta  $k_1, k_2$  chosen as indicated, and numerator terms due to spin suppressed:

We simplify:

$$\not{p}_a + \not{k} + m = \frac{1}{2}(\not{p}_a^+ + \not{k}^+)\gamma^- + \frac{1}{2}(\not{p}_a^- + \not{k}^-)\gamma^+ - (\vec{p}_a + \vec{k}) \cdot \vec{\gamma} + m = \frac{1}{2}Q\gamma^+ + O(Q^0), \quad (3.14a)$$

$$\not{p}_b + \not{k} + m = \frac{1}{2}Q\gamma^- + O(Q^0), \quad (3.14b)$$

where  $\gamma^\pm = \gamma^0 \pm \gamma^3$  and  $\vec{\gamma} = (\gamma^x, \gamma^y)$ . Convenient and frequently used properties of these combinations of  $\gamma$  matrices are

$$\gamma^{-2} = \gamma^{+2} = 0, \quad \{\gamma^\pm, \vec{\gamma}\} = 0, \quad (3.14c)$$

$$\gamma^\pm \vec{\gamma} \vec{\gamma}^\pm = 4\gamma^\pm, \quad \gamma^+ \gamma^- + \gamma^- \gamma^+ = 4.$$

When spinors are present, one may use

$$\gamma^+ u(p_a) = O(m/Q)u(p_a), \quad \gamma^+ \gamma^- u(p_a) = [4 + O(1/Q)]u(p_a), \quad (3.15)$$

$$\bar{u}(p_b)\gamma^- = O(m/Q)\bar{u}(p_b), \quad \bar{u}(p_b)\gamma^+\gamma^- = [4 + O(1/Q)]\bar{u}(p_b).$$

Using these relations, we find immediately

$$N^\mu(Q \rightarrow \infty) = -(\frac{1}{2}Q)^2 \frac{1}{2}\bar{u}(p_b)\gamma^+\gamma^-\gamma^\mu\gamma^+u(p_a) = -2Q^2\bar{u}\gamma^\mu u. \quad (3.16)$$

In the off-shell case we must put instead

$$N^\mu(Q \rightarrow \infty) = -2Q^2(-\frac{1}{4}\gamma^+\gamma^\perp\gamma^-). \quad (3.17)$$

Substituting Eqs. (3.8) and (3.16) into Eq. (3.13) and integrating once with respect to  $Q$ , we have the desired result:

$$\Lambda_{(1)}^\mu = -\left(\frac{e^2}{16\pi^2}\right) \bar{u}\gamma^\mu u \ln^2(Q^2/\mu^2) + O(\ln(Q^2/\mu^2)), \quad (3.18)$$

and a similar result in the off-shell case. In fact we shall always be able to first evaluate the vertex for the (convergent) scalar case and then multiply by the numerator function which describes the spin degrees of freedom with the limit  $Q \rightarrow \infty$  naively taken. One way to view this result is to note that terms in the numerator proportional to  $k$  do not cancel with  $Q^2$ 's in the denominator and are thus asymptotically small when renormalized compared to those terms for which the  $Q^2$ 's in the denominator are cancelled. The details of vertex renormalizations are thereby completely bypassed.

The remaining diagrams of  $O(e^2)$  are those of Fig. 2(b) and Fig. 2(c). These merely generate fermion mass and wave-function renormalizations and can be ignored.<sup>14</sup> Let us turn now to the  $O(e^4)$  diagrams and put to use the lessons we have learned.

$$\Gamma_{(3a)} = \frac{-e^2}{4(2\pi)^6} \int d^2k_1 d^2k_2 \int dk_1^- dk_2^- \int dk_1^+ dk_2^+ (k_1^+ k_1^- - \Delta_1 + i\epsilon)^{-1} (k_2^+ k_2^- - \Delta_2 + i\epsilon)^{-1} (Qk_2^+ - a_2 + i\epsilon)^{-1} \\ \times [Q(k_1^+ + k_2^+) - a_{12} + i\epsilon]^{-1} (Qk_2^- - b_2 + i\epsilon)^{-1} [Q(k_1^- + k_2^-) - b_{12} + i\epsilon]^{-1}, \quad (3.19)$$

where, in analogy to Eq. (3.4),

$$\Delta_i = \vec{k}_i^2 + \mu^2, \\ a_1 = \vec{k}_1^2 + m^2 - m_a^2, \quad a_{12} = (\vec{k}_1 + \vec{k}_2)^2 + m^2 - m_a^2, \\ b_1 = \vec{k}_1^2 + m^2 - m_b^2, \quad b_{12} = (\vec{k}_1 + \vec{k}_2)^2 + m^2 - m_b^2.$$

In writing Eq. (3.19) we have immediately made the approximations of Eq. (3.2) as well as those discussed just before Eq. (3.7); the justification for these can be made just as before. Carrying out the  $k_1^+$  and  $k_2^+$  integrations by contour methods, we have

$$\Gamma_{(3a)} = \frac{e^4}{4(2\pi)^6} \frac{1}{Q^4} \int d^2k_1 d^2k_2 \int_{-\infty}^0 dk_1^- \int_{-\infty}^0 dk_2^- \frac{k_2^-}{(k_2^- - b_2/Q)(k_1^- + k_2^- - b_{12}/Q)} \frac{1}{(\Delta_2 - k_2^- a_2/Q)(k_2^- \Delta_1 + k_1^- \Delta_2 - k_1^- k_2^- a_{12}/Q)}. \quad (3.20)$$

If we were to evaluate the above integral, it is straightforward to see that because of the presence of  $k_2^-$  in the numerator we may safely take the limit  $Q \rightarrow \infty$  in the first denominator factor of the integrand. That is  $k_2^- (k_2^- - b_2/Q)^{-1} - 1$  does not affect the asymptotic behavior in  $Q^2$ , and cannot build up a logarithmic enhancement. This approximation – a very important one in what follows – can be verified by carrying out the plus integrations with no approximations beyond those of Eq. (3.2).

Rather than carrying out further reduction of Eq. (3.20) it is advantageous to stop here and examine the crossed diagram 3(b). We will see that both diagrams have the same asymptotic  $Q$  dependence and that the sum of the two turns out to have a particularly simple form. Labeling the loop momenta as shown and approximating the propagators as in Eq. (3.19) we find, after carrying out the  $k_1^+, k_2^+$  contour integrals,

$$\Gamma_{(3b)} = \frac{e^4}{4(2\pi)^6} \frac{1}{Q^2} \int d^2k_1 d^2k_2 \int_{-\infty}^0 dk_1^- \int_{-\infty}^0 dk_2^- \frac{k_2^-}{(k_1^- - b_1/Q)(k_1^- + k_2^- - b_{12}/Q)} \frac{1}{(\Delta_2 - k_2^- a_2/Q)(k_2^- \Delta_1 + k_1^- \Delta_2 - k_1^- k_2^- a_{12}/Q)}. \quad (3.21)$$

Forming now the combination  $\Gamma_{(3a)} + \Gamma_{(3b)}$ , we have for the integrand common terms multiplied by

$$\left(1 + \frac{k_2^-}{k_1^- + b_1/Q}\right) \frac{1}{(k_1^- + k_2^- - b_{12}/Q)} = \frac{(k_1^- + k_2^- + b_1/Q)}{(k_1^- + b_1/Q)(k_1^- + k_2^- - b_{12}/Q)}. \quad (3.22)$$

Knowing that the small  $k_1^-, k_2^-$  is the only source of (infrared) logarithms in the  $k_{1,2}^-$  integrations, we see that we may further simplify the right-hand side of Eq. (3.22) to

$$\frac{k_1^- + k_2^- + b_1/Q}{(k_1^- + b_1/Q)(k_1^- + k_2^- - b_{12}/Q)} \xrightarrow{Q \rightarrow \infty} (k_1^- + b_1/Q)^{-1}.$$

The integrand,  $I_{a+b}$ , of  $\Gamma_{(3a)} + \Gamma_{(3b)}$  is now, up to constants,

$$I_{a+b} = \left(k_1^- - \frac{b_1}{Q}\right)^{-1} \left(\Delta_2 - \frac{k_2^- a_2}{Q}\right)^{-1} \left(k_2^- \Delta_1 + k_1^- \Delta_2 - k_1^- k_2^- \frac{a_{12}}{Q}\right)^{-1}. \quad (3.23)$$

Our final technique is to symmetrize the expression (3.23) with respect to  $k_1$  and  $k_2$ . This gives, in place of Eq. (3.23)

$$I_{a+b} = \frac{1}{2!} \frac{k_2^- \Delta_1 + k_1^- \Delta_2 - O(1/Q, 1/Q^2)}{k_2^- \Delta_1 + k_1^- \Delta_2 - k_1^- k_2^- \Delta_{12}/Q} \left(k_1^- - \frac{b_1}{Q}\right)^{-1} \left(\Delta_1 - \frac{k_1^- \Delta_1}{Q}\right)^{-1} \left(k_2^- - \frac{b_2}{Q}\right)^{-1} \left(\Delta_2 - \frac{k_2^- \Delta_2}{Q}\right)^{-1}.$$

Again we may selectively set  $Q \rightarrow \infty$  wherever it will not introduce an “infrared” divergence. This brings  $I_{a+b}$  to its final form:

$$I_{a+b} = \frac{1}{2!} \left(k_1^- - \frac{b_1}{Q}\right)^{-1} \left(\Delta_1 - \frac{k_1^- a_1}{Q}\right)^{-1} \left(k_2^- - \frac{b_2}{Q}\right)^{-1} \left(\Delta_2 - \frac{k_2^- a_2}{Q}\right)^{-1}. \quad (3.24)$$

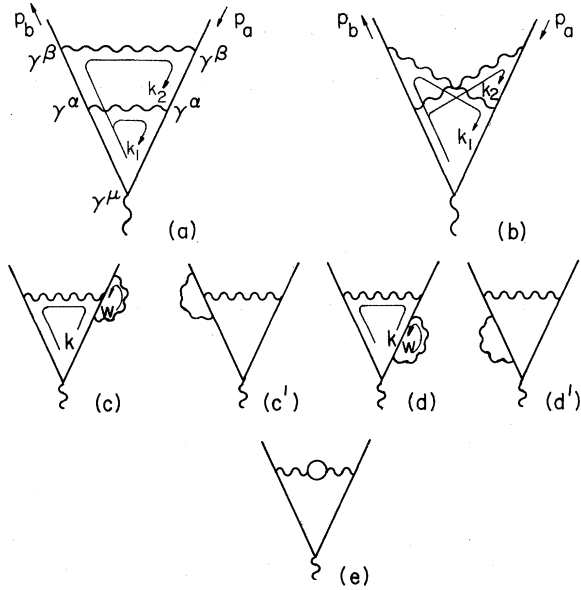


FIG. 3. The relevant fourth-order diagrams. (a) and (b) are asymptotically leading and sum to a simple form. (c) and (d) are not asymptotically leading. Furthermore the sum of their leading terms cancels. (e) is separately gauge-invariant.

In obtaining the form of Eq. (3.24) we have achieved the remarkable result of completely decoupling the remaining  $k_1$  and  $k_2$  integrals. Further,  $I_{a+b}$  is, except for the over-all  $1/2!$ , precisely the square of the lowest-order result, Eq. (3.7). Thus

$$\Gamma_{(3a)+} \Gamma_{(3b)} = \frac{1}{2!} (\Gamma^{(1)})^2.$$

The numerator spin factors for diagrams 3(a) and 3(b) are equal as  $Q \rightarrow \infty$ . This is clear since they differ only in the  $k_1, k_2$  variables which we drop asymptotically. Thus to leading order,

$$\begin{aligned} N_{(3a)}^\mu &\cong N_{(3b)}^\mu \cong \bar{u}(p_b) \gamma^\beta \not{p}_b \gamma^\alpha \not{p}_b \gamma^\mu \not{p}_a \gamma^\alpha \not{p}_a \gamma^\beta u(p_a) \\ &= (Q/2)^4 \bar{u}(p_b) \gamma^+ \gamma^- \gamma^+ \gamma^- \gamma^+ \gamma^- \gamma^+ \gamma^- u(p_a) \\ &= (-2Q^2)^2 \bar{u}(p_b) \gamma^+ u(p_a). \end{aligned} \quad (3.25)$$

Hence, our final fourth-order result for diagrams 3(a) and 3(b) is

$$\Lambda_{(3a+3b)}^\mu = \frac{1}{2!} (-2Q^2 \Gamma^{(1)})^2 \bar{u}(p_b) \gamma^+ u(p_b); \quad (3.26)$$

off-shell,  $\bar{u} \gamma^+ u \rightarrow -\frac{1}{4} \gamma^+ \gamma^+ \gamma^-$ . [The generalization of the trick we used in second order to show that, after renormalization, the integration region  $|k_{1,2}^\nu| \geq \epsilon Q$  is unimportant is simply to consider  $\Lambda^\mu$  differentiated three times with respect to  $Q$ . After differentiation, both the crossed- and more troublesome uncrossed-ladder diagrams will have

the desired convergence in all loop integrations. In order  $e^2$ , when we integrated to find the vertex itself, the single (unknown) constant of integration was small compared to  $\ln^2(Q^2/\mu^2)$ . This time there is the possibility of an additive polynomial of up to second order in  $Q^2$ . Weinberg's theorem,<sup>15</sup> however, assures us immediately that the additive polynomial can actually have no higher than constant terms. Hence our result.]

To complete the fourth-order calculation it remains to show that the vertex corrections, Figs. 3(c) and 3(c') and the fermion self-energy insertions, Figs. 3(d) and 3(d'), are asymptotically small compared to what we have already calculated. We will see that separately these diagrams contribute  $\sim \ln^3 Q^2$ , and hence are down by one power of  $\ln Q^2$  compared to diagrams 3(a) and 3(b). However, it is further true that the  $\ln^3 Q^2$  cancels between diagrams 3(c) and 3(d) [and between 3(c') and 3(d')], leaving a contribution of at most  $O(\ln^2 Q^2)$ .

The vacuum polarization insertion, Fig. 3(e), is itself gauge invariant and will be discussed last.

To demonstrate these points, it turns out to be more convenient to use the spectral function representation for the self-energy insertions and to exploit the information contained in the Ward-Takahashi identity about the vertex, rather than to calculate straightforwardly as we have previously done. Let us begin with the self-energy insertion, Fig. 3(d); Fig. 3(d') gives an identical contribution.

This diagram is the same as the leading  $O(e^2)$  diagram [(Fig. 2(a)) except for the replacement in the right-hand fermion line

$$\frac{i(\not{p}+m)}{p^2-m^2} \rightarrow \frac{i(\not{p}+m)}{p^2-m^2} [-i\Sigma(p)] \frac{i(\not{p}+m)}{p^2-m^2}, \quad (3.27)$$

where  $p \equiv p_a + k$ . The self-energy  $\Sigma(p)$  has the general form

$$\Sigma(p) = A(p^2)(\not{p}-m) + B(p^2), \quad (3.28)$$

where  $A$  and  $B$  are divergent functions in perturbation theory. The statement that  $m$  is the physical fermion mass requires that

$$\Sigma(p)u(p) = 0, \quad p^2 = m^2;$$

hence

$$B(m^2) = 0. \quad (3.29)$$

It is convenient to introduce the following decomposition:

$$\begin{aligned} A(p^2) &\equiv A(m^2) + (p^2 - m^2) \tilde{A}(p^2) \\ &\equiv A(m^2) + (p^2 - m^2) \tilde{A}(m^2) + (p^2 - m^2)^2 \bar{A}(p^2) \end{aligned} \quad (3.30)$$

and similarly for  $B(p^2)$ . The quantities  $\bar{A}$ ,  $\bar{A}$ , and  $\bar{B}$  are finite in perturbation theory. In terms of these quantities we may rewrite the right-hand side of Eq. (3.27):

$$\frac{i(\not{p}+m)\Sigma(\not{p})(\not{p}+m)}{(p^2-m^2)^2} = \frac{i(\not{p}+m)}{p^2-m^2} L^2 + i(\not{p}+m)[\bar{A}(p^2) + 2m\bar{B}(p^2)] + \bar{B}(p^2), \quad (3.31)$$

where the constant  $L^2 = A(m^2) + 2m\bar{B}(m^2) = 1 - Z_2^{-1}$  is recognized as the fermion wave-function renormalization.

The first term on the right-hand side of Eq. (3.31) clearly contributes the same  $O(\ln^2 Q^2)$  as the  $O(e^2)$  diagram, Fig. 2(a); it is simply part of the coupling-constant renormalization.<sup>16</sup> In the remaining part of Eq. (3.31) only the term  $\sim \not{p}$  is important; recall  $\not{p} \sim \frac{1}{2} Q \gamma^+$  at large  $Q$ .

We now write a dispersion relation (spectral

representation) for the quantity  $\bar{A}(p^2) + 2m\bar{B}(p^2)$ ,

$$\bar{A}(p^2) + 2m\bar{B}(p^2) = \frac{1}{\pi} \int_{(m+\mu)^2}^{\infty} \frac{d\sigma^2 \rho(\sigma^2)}{\sigma^2 - p^2}, \quad (3.32)$$

where<sup>17</sup> to  $O(e^2)$

$$\rho_{(a)}(\sigma^2) = - \left( \frac{e^2}{4\pi} \right) \frac{\Delta^{1/2}(\sigma^2, m^2, \mu^2)}{\sigma^2(\sigma^2 - m^2)^2} \times \left[ (\sigma^2 - 3m^2) - (\sigma^2 + m^2) \frac{\sigma^2 + \mu^2 - m^2}{2\sigma^2} \right] \quad (3.33)$$

and

$$\Delta(x, y, z) = x^2 + y^2 + z^2 - 2xy - 2xz - 2yz.$$

As  $\sigma^2 \rightarrow \infty$ ,  $\rho(\sigma^2) \sim \sigma^{-2}$ , guaranteeing that the dispersion relation (3.32) is convergent.

The spectral form, Eq. (3.22), is extremely convenient since we may immediately write down the contribution of diagram 3(d) in terms of our lower-order result, Eq. (3.7),

$$\Lambda_{(3d)}^\mu = \frac{1}{\pi} \int_{(m+\mu)^2}^{\infty} d\sigma^2 \rho(\sigma^2) \frac{e^2}{2(2\pi)^3} \int d^2 k \int_{-\infty}^0 dk^- \frac{(-2Q^2)}{(k^- Q - b)[k^-(\vec{k}^2 + \sigma^2 - m_a^2) - Q\Delta]}. \quad (3.34)$$

The precise value of this integral at large  $Q^2$  depends on the value of the external masses  $m_a^2$  and  $m_b^2$ . The result is always  $\sim \ln^3 Q^2$ , however. For simplicity, let us illustrate the on-shell case  $m_a^2 = m_b^2 = m^2$  only. Carrying out the  $k$  integrations in Eq. (3.34), as discussed in Appendix A, we have

$$\Lambda_{(3d)}^\mu = \frac{e^2}{(2\pi)^3} \int_{(m+\mu)^2}^{\infty} d\sigma^2 \rho(\sigma^2) \frac{Q^2 \ln[(\sigma^2 - m^2)/Q^2]}{\sigma^2 - Q^2 - m^2} \left[ \ln\left(\frac{Q^2}{\mu^2}\right) + \ln\left(\frac{\sigma^2 - m^2}{\mu^2}\right) \right]. \quad (3.35)$$

The dominant contribution to  $\Gamma_{(3d)}^\mu$  comes from the range of  $\sigma^2$ , where  $\rho(\sigma) \sim 1/\sigma^2$  and  $\sigma^2 < Q^2$ ; more precisely,  $\mu^2/\epsilon' < \sigma^2 < \epsilon Q^2$ ,  $\epsilon, \epsilon' \ll 1$ . The contribution from all other  $\sigma^2$  regions is a  $\ln Q^2$  or more smaller. Thus

$$\Lambda_{(3d)}^\mu \cong \frac{1}{\pi} \left( \frac{e^2}{8\pi^2} \right) \int_{\mu^2/\epsilon'}^{\epsilon Q^2} d\sigma^2 \left( -\frac{e^2}{4\pi} \right) \frac{1}{2} \frac{1}{\sigma^2} \ln\left(\frac{\sigma^2}{Q^2}\right) \left[ \ln\left(\frac{Q^2}{\mu^2}\right) + \ln\left(\frac{\sigma^2}{\mu^2}\right) \right] \cong \frac{10}{3} \left( \frac{e^2}{16\pi^2} \right)^2 \ln^3\left(\frac{Q^2}{\mu^2}\right) + O(\ln^2(Q^2/\mu^2)). \quad (3.36)$$

Let us turn now to the vertex correction, Fig. 3(c). It contributes

$$\Lambda_{(3c)}^\mu = \frac{-i}{(2\pi)^4} \int d^4 k \frac{\bar{u}(p_b) \gamma^\alpha (\not{p}_b + \not{k} + m) \gamma^\mu (\not{p}_a + \not{k} + m) \Lambda_{(1)}^\alpha(k^2, (p_a + k)^2, m^2) u(p_a)}{(k^2 - \mu^2)[(p_b + k)^2 - m^2][(p_a + k)^2 - m^2]} \cong \frac{-i}{(2\pi)^4} \left( \frac{Q}{4} \right) \int d^4 k \frac{\bar{u}(p_b) \gamma^+ \gamma^- \gamma^\mu (\not{p}_a + \not{k} + m) \Lambda_{(1)}^-(p_a)}{(k^2 - \mu^2)(Qk^- - b)[(p_a + k)^2 - m^2]}, \quad (3.37)$$

where for convenience we again have illustrated the on-shell case. In Eq. (3.37)  $\Lambda_{(1)}^\alpha$  is the  $O(e^2)$  (half) off-shell vertex previously studied in its asymptotic form in Eq. (3.18). [See also Eq. (A4).] We define  $p \equiv p_a + k$  and use Eq. (2.4) to write the general structure

$$\Lambda^\alpha(k^2, (p+k)^2, m^2) u(p_a) = \left( \frac{\not{p} + m}{2m} \right) (\gamma^\alpha \mathcal{F}_1 + i\sigma^{\alpha\nu} k_\nu \mathcal{F}_2 + k^\alpha \mathcal{F}_3) u(p_a) + \left( \frac{-\not{p} + m}{2m} \right) (\gamma^\alpha \mathcal{F}_{10} + i\sigma^{\alpha\nu} k_\nu \mathcal{F}_{11} + k^\alpha \mathcal{F}_{12}) u(p_a). \quad (3.38)$$

The denominators in Eq. (3.37) are identical to the  $O(e^2)$  vertex. We saw there that the dominant  $Q^2$  behavior came from the region  $(p_a + k)^2 \equiv p^2 \approx m^2$  and large  $\vec{k}^2$  ( $\mu^2 < \vec{k}^2 < Q^2$ ). We learned, too, that in precisely this region all but the Dirac ( $\gamma^\alpha$ ) type form factors fall at large photon masses and thus we may use in Eq. (3.27) the bounds

$$|\mathcal{F}_i(k^2, p^2, m^2)| \leq \text{const} \frac{1}{|\vec{k}^2| + \mu^2}, \quad i = 2, 3, 11, 12.$$

Besides suppression at large  $k^2$  that this implies, the coefficients of these form factors in the numerator of Eq. (3.37) bring about further suppression of the large  $Q^2$  behavior.  $\mathcal{F}_3$  and  $\mathcal{F}_{12}$  have a coefficient  $k^-$  which suppresses an infrared logarithm.  $\mathcal{F}_2$  and  $\mathcal{F}_{11}$  have coefficients  $k^-$  or  $\vec{k}$  which suppress a logarithm or vanish by symmetry, respectively. Thus all contributions from the  $\mathcal{F}_{2,3,11,12}$  terms to Eq. (3.37) are safely  $\leq O(\ln^2 Q^2)$ .

Retaining only  $\mathcal{F}_1$  and  $\mathcal{F}_{10}$ , the numerator in Eq. (3.37) may be simplified to

$$\begin{aligned} & -\frac{1}{2}(\frac{1}{2}Q)\bar{u}(p_b)\gamma^+\gamma^-\left[(\gamma^\mu\frac{1}{2}Q\gamma^+)\mathcal{F}_1\gamma^- \right. \\ & \quad \left. + \left(\frac{p^2 - m^2}{2m}\right)(\mathcal{F}_1 - \mathcal{F}_{10})\gamma^\mu\gamma^-\right]u(p_a). \end{aligned} \quad (3.39)$$

The first term in this expression is, except for the factor of  $\mathcal{F}_1$ , identical to the  $O(e^2)$  calculation ( $\gamma^+\gamma^\mu\gamma^- = \gamma^+\gamma^1\gamma^-$ ); the second term we shall see is small.<sup>18</sup>

First we write the generalized Ward-Takahashi identity for one particle on-shell,

$$k^\alpha \Lambda^\alpha(k^2, p^2, m^2)u(p_a) = [\not{p} - m - \Sigma(p)]u(p_a), \quad (3.40)$$

relating the divergence of the vertex to the self-energy function. Substituting the general forms from Eqs. (3.28) and (3.38), one finds two independent equations which can be solved to yield<sup>19</sup>

$$\begin{aligned} & -(p^2 - m^2)\mathcal{F}_1 = (p^2 - m^2)A(p^2) + 2mB(p^2) \\ & \quad + \frac{k^2}{2m}[(p^2 + 3m^2)\mathcal{F}_3 - (p^2 - m^2)\mathcal{F}_{12}] \\ & -(p^2 - m^2)(\mathcal{F}_1 - \mathcal{F}_{10}) = 2m[B(p^2) + k^2\mathcal{F}_3]. \end{aligned} \quad (3.41)$$

These equations may now be inserted into the numerator of Eq. (3.37), Eq. (3.39). The  $\mathcal{F}_3$  and  $\mathcal{F}_{12}$  terms in this numerator, by arguments identical to those already presented, give contributions to  $\Lambda_{(3c)}^\mu$  no larger than  $O(\ln^2(Q^2/\mu^2))$ . Therefore we drop them for the remainder of the discussion.<sup>20</sup> The combination  $(p^2 - m^2)(\mathcal{F}_1 - \mathcal{F}_{10})$  which appears in Eq. (3.39) is now given by  $-2mB(p^2)$ , which is by comparison a full power of  $Q$  smaller than the  $\mathcal{F}_1$  term in Eq. (3.39).

Now compare  $\mathcal{F}_1$  as given by Eq. (3.41) with the terms which appear in the same position in the expression for the diagram 3(d) [see Eq. (3.31)]. We see immediately that

$$\Lambda_{(3c)}^\mu = -\Lambda_{(3d)}^\mu + O(\ln^2(Q^2/\mu^2)), \quad (3.42)$$

where the  $O(\ln^2(Q^2/\mu^2))$  term comes from all the  $\mathcal{F}_i$  ( $i = 2, 3, 11, 12$ ) we have neglected. Thus we have established the very useful result that while separately  $\Lambda_{(3c)}^\mu$  and  $\Lambda_{(3d)}^\mu$  are  $\sim \ln^3(Q^2/\mu^2)$ , the sum  $\Lambda_{(3c)}^\mu + \Lambda_{(3d)}^\mu$  is  $\sim \ln^2 Q^2$ . Clearly, the same applies to  $\Lambda_{(3c')}^\mu$  and  $\Lambda_{(3d')}^\mu$ .

Finally consider the vacuum polarization insertion, Fig. 3(e). Using the same spectral techniques that we employ for fermion self-energy insertions, one has after renormalization

$$\Gamma_{(3e)}^\mu = \frac{1}{\pi} \int_{4m^2}^{\infty} d\sigma^2 \rho_{VP}(\sigma^2) (-2Q^2) \Gamma^{(1)}(\mu^2 - \sigma^2), \quad (3.43)$$

where  $\rho_{VP} \rightarrow -(e^2/12\pi)\sigma^{-2}$  as  $\sigma^2 \rightarrow \infty$ . The asymptotic contribution comes from  $(1/\epsilon')\mu^2 < \sigma^2 < \epsilon Q^2$  and is

$$\Gamma_{(3e)}^\mu = -\left(\frac{e^2}{16\pi^2}\right)^2 \frac{4}{9} \ln^3(Q^2/\mu^2) \bar{u}\gamma^1 u. \quad (3.44)$$

#### IV. THE GENERAL CASE

In this section we consider the general case of  $n$  photons exchanged across the vertex, permuted in all possible ways. The diagrams are shown in Fig. 4. As in the second-order case, we first perform contour integrations over the  $k_i^+$ . Since the  $k_i^+$  appear in the photon propagators and in the right-hand fermion propagators only (they do not appear in the left-hand fermion propagators because the left-hand fermion line carries large plus component  $Q$  compared to which all additive  $k_i^+$  may be neglected), we label all the diagrams such that the order of the  $k_i$  loops are the same for the right-hand side of the vertex. This is illustrated in Fig. 4. Then the contour integrals over the  $k_{i+}$  are the same for *all* diagrams. From this point the proof proceeds in two steps. First, we sum over all the diagrams to see that a great simplification occurs. Second, we symmetrize the resultant sum to completely decouple the integrand and show that the integral is the product of the single exchange integrals.

Since we may ignore the  $k_i$  in the numerators, these numerators will be the same for all diagrams. The numerator functions we write in analogy with the numerator of Eq. (3.16) or with Eq. (3.25):

$$N_{(n)}^\mu = (-1)^n \bar{u}(p_b) \gamma^{\alpha n} (p_b + k_i + m) \gamma^{\alpha n-1} (p_b + k_i + k_j + m) \gamma^{\alpha n-2} \cdots \gamma^{\alpha 1} \left( p_b + \sum_{i=1}^n k_i + m \right) \gamma^\mu \left( p_b + \sum_{i=1}^n k_i + m \right) \\ \times \gamma^{\alpha 1} \left( p_a + \sum_{i=2}^n k_i + m \right) \gamma^{\alpha 2} \cdots \gamma^{\alpha n-1} (p_a + k_n + m) \gamma^{\alpha n} u(p_a). \quad (4.1)$$

We have

$$(p_b + \sum k_i + m) \approx \frac{1}{2} Q \gamma^-, \quad (p_a + \sum k_i + m) \approx \frac{1}{2} Q \gamma^+,$$

and

$$\gamma^{\alpha j} \cdots \gamma^{\alpha i} \rightarrow \frac{1}{2} \gamma^+ \cdots \gamma^-.$$

Then

$$N_{(n)}^\mu = (-1)^n 2^{-3n} Q^{2n} u(p_b) \gamma^+ \gamma^- \gamma^+ \cdots \gamma^+ \gamma^- \gamma^\mu \gamma^+ \gamma^- \gamma^+ \cdots \gamma^- u(p_a).$$

In the above equation, there are  $n$   $\gamma^-$ 's to the left of  $\gamma^\mu$  and  $n$   $\gamma^+$ 's to the right of  $\gamma^\mu$ . We now use our reduction techniques to show that

$$N_{(n)}^\mu = (-1)^n 2^n Q^{2n} \bar{u}(p_b) \gamma^\perp u(p_a), \quad (4.2)$$

where again  $\gamma^\mu$  has a perpendicular component only. Thus, after renormalization,<sup>21</sup> we have asymptotically

$$\Lambda_{(n)i}^\mu = (-2Q^2)^n \Gamma_i^{(n)} \bar{u}(p_b) \gamma^\perp u(p_a), \quad (4.3)$$

where  $\Gamma_i^{(n)}$  is the vertex for the spinless case and  $i$  describes any of the  $n!$  diagrams in Fig. 4. (Off shell, replace  $\bar{u} \gamma^\perp u \rightarrow -\frac{1}{4} \gamma^+ \gamma^\perp \gamma^-$ .)

For definiteness, let us look at the straight ladder, which is the first diagram in Fig. 4. This expression is

$$\Gamma^{(n)} = (-ie^2)^n \int \frac{\prod d^4 k_i}{(2\pi)^{4n}} \left[ \prod (k_i^2 - \mu^2 + i\epsilon) \right]^{-1} \left\{ [(p_b + k_n)^2 - m^2 + i\epsilon] [(p_b + k_n + k_{n-1})^2 - m^2 + i\epsilon] \cdots \right. \\ \left. \times \left[ \left( p_b + \sum_{i=1}^n k_i \right)^2 - m^2 + i\epsilon \right] \right\}^{-1} \left\{ [(p_a + k_n)^2 - m^2 + i\epsilon] [(p_a + k_n + k_{n-1})^2 - m^2 + i\epsilon] \cdots \left[ \left( p_a + \sum_{i=1}^n k_i \right)^2 - m^2 + i\epsilon \right] \right\}^{-1} \\ = \left( \frac{-e^2}{(2\pi)^4} \right)^n Q^{-2n} \frac{1}{2^n} \int \prod d^2 k_i \left( \prod \int \frac{dk_i^-}{k_i^-} \right) \left[ \left( k_n^- - \frac{b_n}{Q} \right) \left( k_n^- + k_{n-1}^- - \frac{b_{n,n-1}}{Q} \right) \cdots \left( \sum_{i=1}^n k_i^- - \frac{b_{1,2,\dots,n}}{Q} \right) \right]^{-1} \\ \times \int \prod dk_i^+ \left[ \prod_{i=1}^n \left( k_i^+ - \frac{\Delta_i}{k_i^+} + \frac{i\epsilon}{k_i^+} \right) \right]^{-1} \left[ \left( k_n^+ - \frac{a_n}{Q} + i\epsilon \right) \left( k_n^+ + k_{n-1}^+ - \frac{a_{n,n-1}}{Q} + i\epsilon \right) \cdots \left( \sum_{i=1}^n k_i^+ - \frac{a_{1,2,\dots,n}}{Q} + i\epsilon \right) \right]^{-1}. \quad (4.4)$$

All but the first term in square brackets of Eq. (4.4) is common to every diagram of Fig. 4; for the various diagrams this first term varies in having all combinations of the  $k_i$  which appear in the following sense. Choose a particular  $k_i^-$  for the first term ( $k_i^- - b/Q$ ), a second  $k_j^-$  to accompany  $k_i^-$  in the second term ( $k_i^- + k_j^- - b_{ij}/Q$ ), etc., until last term is  $(\sum_{i=1}^n k_i^- - b_{1,2,\dots,n}/Q)$ . The factor  $b_{i,j,\dots,k}$  which appears in Eq. (4.4) is just  $(\vec{k}_i + \vec{k}_j + \cdots + \vec{k}_k)^2 + m^2 - m_b^2$ , and similar for  $a_{i,j,\dots,k}$ .

We can now perform the integrations over the  $k_i^+$  by contour methods. We must restrict  $k_i^- < 0$  in order to get a contribution at all. Given this restriction, we close the  $k_i^+$  contour above to pick up the poles at  $k_i^+ = \Delta_i/k_i^+ + i\epsilon$ . The result is

$$\Gamma_1^{(n)} = \left( \frac{-e^2}{(2\pi)^3} \right)^n Q^{-2n} \frac{1}{2^n} \int \prod d^2 k_i \left( \prod \int_{-\infty}^0 \frac{dk_i^-}{k_i^-} \right) \left[ \left( k_n^- - \frac{b_n}{Q} \right) \left( k_n^- + k_{n-1}^- - \frac{b_{n,n-1}}{Q} \right) \cdots \left( \sum_{i=1}^n k_i^- - \frac{b_{1,2,\dots,n}}{Q} \right) \right]^{-1} \\ \times \left[ \left( \frac{\Delta_n}{k_n^-} - \frac{a_n}{Q} \right) \left( \frac{\Delta_n}{k_n^-} + \frac{\Delta_{n-1}}{k_{n-1}^-} - \frac{a_{n,n-1}}{Q} \right) \cdots \left( \sum_{i=1}^n \frac{\Delta_i}{k_i^-} - \frac{a_{1,2,\dots,n}}{Q} \right) \right]^{-1}. \quad (4.5)$$

Let us now consider the summation of all the  $n!$  diagrams of Fig. 4. Each diagram has a form like Eq. (4.5), but with different permutations of the  $k_i^-$  appearing in the first square bracket. Denote this square bracket by  $G_i^{(n)}$ , where  $i$  labels the particular diagram being studied. Let us consider the summation of the  $G_i^{(n)}$  over  $i$ . In doing so, we find when we rationalize that there are  $\Delta_{i,j,\dots,k}/Q$  terms in the numerator; these we may safely ignore as not contributing to the leading behavior. After some algebra we find that the remainder of the numerator is just

$$\left(\prod_{i \neq j} (k_i^- + k_j^-)\right) \left(\prod_{i \neq j \neq l} (k_i^- + k_j^- + k_l^-)\right) \cdots \left(\sum_{i=1}^n k_i^-\right).$$

Thus

$$\sum_{i=1}^{n!} G_i^{(n)} = \left\{ \left[ \prod_{i=1}^n \left(k_i^- - \frac{b_i}{Q}\right) \right] \left[ \prod_{i \neq j} \left(k_i^- + k_j^- - \frac{b_{i,j}}{Q}\right) \right] \cdots \left( \sum_{i=1}^n k_i^- - \frac{b_{1,2,\dots,n}}{Q} \right) \right\}^{-1} \\ \times \left( \prod_{i \neq j} (k_i^- + k_j^-) \right) \left( \prod_{i \neq j \neq l} (k_i^- + k_j^- + k_l^-) \right) \cdots \left( \sum_{i=1}^n k_i^- \right).$$

By our previous arguments, we may in determining the leading behavior replace

$$(k_i^- + k_j^-) \left(k_i^- + k_j^- - \frac{b_{i,j}}{Q}\right)^{-1}, \dots, \sum_{i=1}^n k_i^- \left(\sum_{i=1}^n k_i^- - \frac{b_{1,2,\dots,n}}{Q}\right)^{-1}$$

by 1. This leaves us with

$$\sum_{i=1}^{n!} G_i^{(n)} = \prod_{i=1}^n \left(k_i^- - \frac{b_i}{Q}\right)^{-1}, \tag{4.6}$$

which is a great simplification for the sum of all diagrams of Fig. 4.

Finally we may perform a symmetrization on the remaining unsymmetrical piece of  $\sum_{i=1}^{n!} \Gamma_i^{(n)}$ . Since the sum over the  $G_i^{(n)}$  is, according to Eq. (4.6), symmetrical, the only remaining unsymmetrical piece is the second term in square brackets in Eq. (4.5), which we shall call  $H_i^{(n)}$ . In this case the  $i$  labels the particular arbitrary choice of the loop variable ordering along the right-hand fermion leg of Fig. 4. As for  $G_i^{(n)}$ , when we sum over the  $H_i^{(n)}$  and rationalize, we find  $a_{i,j,\dots,k}/Q$  terms in the numerator, which we discard. The remainder of the numerator is

$$\left[ \prod_{i \neq j} \left(\frac{\Delta_i}{k_i^-} + \frac{\Delta_j}{k_j^-}\right) \right] \left[ \prod_{i \neq j \neq k} \left(\frac{\Delta_i}{k_i^-} + \frac{\Delta_j}{k_j^-} + \frac{\Delta_k}{k_k^-}\right) \right] \cdots \left(\sum_{i=1}^n \frac{\Delta_i}{k_i^-}\right).$$

Thus

$$\sum_{i=1}^{n!} H_i^{(n)} = \left\{ \left[ \prod_{i \neq j} \left(\frac{\Delta_i}{k_i^-} - \frac{a_i}{Q}\right) \right] \left[ \prod_{i \neq j} \left(\frac{\Delta_i}{k_i^-} + \frac{\Delta_j}{k_j^-} - \frac{a_{i,j}}{Q}\right) \right] \cdots \left( \sum_{i=1}^n \frac{\Delta_i}{k_i^-} - \frac{a_{1,2,\dots,n}}{Q} \right) \right\}^{-1} \\ \times \left[ \prod_{i \neq j} \left(\frac{\Delta_i}{k_i^-} + \frac{\Delta_j}{k_j^-}\right) \right] \left[ \prod_{i \neq j \neq k} \left(\frac{\Delta_i}{k_i^-} + \frac{\Delta_j}{k_j^-} + \frac{\Delta_k}{k_k^-}\right) \right] \cdots \left(\sum_{i=1}^n \frac{\Delta_i}{k_i^-}\right).$$

Once again, we may let

$$\left(\frac{\Delta_i}{k_i^-} + \frac{\Delta_j}{k_j^-}\right) \left(\frac{\Delta_i}{k_i^-} + \frac{\Delta_j}{k_j^-} - \frac{a_{i,j}}{Q}\right)^{-1}, \dots, \left(\sum_{i=1}^n \frac{\Delta_i}{k_i^-}\right) \left(\sum_{i=1}^n \frac{\Delta_i}{k_i^-} - \frac{a_{1,2,\dots,n}}{Q}\right)^{-1} \rightarrow 1,$$

leaving

$$\sum_{i=1}^{n!} H_i^{(n)} = \prod_{i=1}^n \left(\frac{\Delta_i}{k_i^-} - \frac{a_i}{Q}\right)^{-1} = \prod_{i=1}^n k_i^- \left(\Delta_i - \frac{a_i k_i^-}{Q}\right)^{-1}. \tag{4.7}$$

The factor  $k_1^- k_2^- \dots k_n^-$  cancels with an identical factor in the denominator of Eq. (4.5). Finally we must accompany the summation of  $H_i^{(n)}$  by a factor  $1/n!$ . Thus the sum over all diagrams of Fig. 4 is

$$\Gamma^{(n)} = \frac{1}{n!} \left(\frac{e^2}{2Q^2(2\pi)^3}\right)^n \int \prod_{i=1}^n d^2 k_i \int_{-\infty}^0 \prod_{i=1}^n dk_i^- \left(k_i^- - \frac{b_i}{Q}\right)^{-1} \left(\frac{k_i^- a_i}{Q} - \Delta_i\right)^{-1} \\ = \frac{1}{n!} (\Gamma^{(1)})^n. \tag{4.8}$$

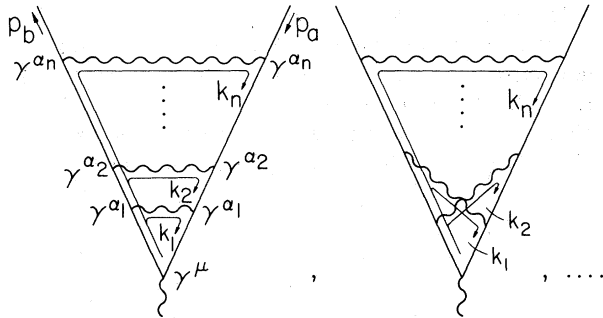


FIG. 4. The leading diagrams in arbitrary order are photons exchanged across the main vertex permuted in all possible ways. These diagrams sum to a simple form.

When we put in the numerator function Eq. (4.2), we find the asymptotic form of the Dirac form factor in  $n$ th order:

$$\mathcal{F}_1^{(n)} = \frac{1}{n!} (-\Phi_0)^n, \tag{4.9}$$

where  $\Phi_0 = +2Q^2\Gamma^{(1)}(Q^2, m_b^2, m_a^2)$ , which sums to the exponential form

$$\mathcal{F}_1 = e^{-\Phi_0}. \tag{4.10}$$

The argument of the exponential now depends upon the value of  $\Phi_0$ ; we evaluate this quantity in the off-shell (Sudakov) case or in the on-shell case in Appendix A. Sudakov's result<sup>8</sup> holds in the first case, and in the on-shell case

$$F_1(Q^2) = \exp\left[-\frac{e^2}{16\pi^2} \ln^2(Q^2/\mu^2)\right]. \tag{4.11}$$

Let us now briefly turn to the question of "radiative corrections" without pair production, of which some examples are shown in Fig. 5. The general technique for treating such a diagram [Fig. 5(a) for example] is to use a spectral representation for the self-energy pieces and Ward-Takahashi identities

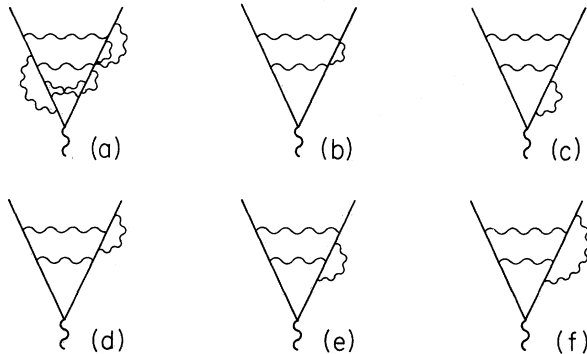


FIG. 5. (a) A general type of diagram without pair production. (b)–(f) A set of diagrams whose individual leading contributions may cancel among themselves in analogy with the diagrams of Fig. 3(c) and 3(d).

to relate the vertex corrections to these self-energy pieces. It is then straightforward to see, as we saw in Sec. III, that although the leading power dependence of these individual diagrams matches that of the exchange diagrams, namely, no overall factors of  $Q$ , the number of powers of  $\ln(Q^2/\mu^2)$  for a given power of  $e^2$  is at least one less. We saw in Sec. III, however, a further cancellation between a gauge-related set of corrections to a given fermion line, namely Figs. 3(c) and 3(d). In this case the  $e^4 \ln^3(Q^2/\mu^2)$  cancelled, leaving a contribution which is at most  $O(e^4 \ln^2(Q^2/\mu^2))$ , i.e., the same number of  $\ln$ 's as the vertex with one line across. Although we have not yet rigorously established such a cancellation in general, calculations beyond those presented here lead us to conjecture that such a cancellation does indeed occur. As an example, the  $O(e^6 \ln^3(Q^2/\mu^2))$  behavior of the individual diagrams of Figs. 5(b)–5(f) would cancel, leaving  $O(e^6 \ln^4(Q^2/\mu^2))$  for these corrections.

Finally, we consider the effect of vacuum polarization insertions on the photon lines. For each such insertion the contribution is one order of  $\ln Q^2$  smaller than the ladder diagrams of the same power of the coupling constant. This follows immediately from the argument presented at the end of Sec. III.

Furthermore, the effect of vacuum polarization insertions in the photon lines done in all possible ways continues to exponentiate; only  $\Phi$  changes. For example, if we include at most one insertion per photon line, our work shows that the appropriate  $\Phi$  is, for the on-shell case,

$$\Phi = \Phi_0 + \Phi_{VP} = \frac{e^2}{16\pi^2} \ln^2(Q^2/\mu^2) + \left(\frac{e^2}{16\pi^2}\right)^2 \frac{4}{9} \ln^3(Q^2/\mu^2). \tag{4.12}$$

We have not yet included photon-photon scatter-

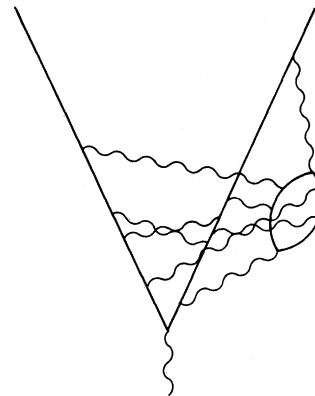


FIG. 6. A diagram with interacting fermions from pair production; alternatively, a diagram with a photon-photon interaction insertion. We do not consider such diagrams.

ings, an example of which is shown in Fig. 6.

### V. ALTERNATE PATHWAYS AND OTHER FIELD THEORIES

In this section we show how the approximations we have developed have a natural interpretation in terms of pathways for infinite momentum. In terms of this language we qualitatively discuss the possible exponentiation of the vertex function in spinless field theories such as  $\lambda\varphi^3$ .

We have seen, when  $Q^2$  is much larger than any of the internal and external masses, that if a line carries loop momentum  $k^+$  ( $k^-$ ) in addition to a large  $+$  ( $-$ ) component  $Q$  we may ignore  $k^+$  ( $k^-$ ) compared to  $Q$ . That a particular internal line is carrying this large  $\pm$  momentum allows us to "follow" it through the diagram. Recalling  $q^\mu = (Q, \vec{0}, -Q)$ , we see that a large  $q^+ = Q$  enters the diagram at the  $\gamma^\mu$  vertex and exits in fermion line  $b$ ,  $p_b^+ \cong Q$ . Similarly, large negative momentum  $p_a^- \cong Q$  enters in fermion line  $a$  and flows out of the  $\gamma^\mu$  vertex,  $q^- = -Q$ .<sup>22</sup> One sometimes speaks similarly of pathways in the more standard Feynman parameter approach to asymptotic behavior, but the connection to a visualizable path seems to us somewhat remote. This is especially so for the vertex function since, in the Feynman parameter approach, the dominant contributions come from "singular configurations," in the language of Tiktopoulos.<sup>23</sup>

In addition, we can see that an individual propagator must not carry both large  $+$  and large  $-$  components, because then its denominator will be proportional to  $Q^2$  which cannot be compensated by numerators  $Q$ 's (if any). This is well known from previous infinite-momentum work.

So far we have studied the vector-spinor field theory (massive QED). In this theory the choice of infinite momentum pathways is more or less obvious,<sup>22</sup> because if the path follows a fermion propagator, there is a single power of the large momentum  $Q$  in the denominator and a single power in the numerator which asymptotically cancel one another, leaving only logarithmic structure. On the other hand, if the path follows a photon propagator there is a power of  $Q$  in the denominator and no compensating  $Q$  in the numerator ( $g^{\mu\nu}$  gauge).

In a field theory with only one type of particle, one must consider all the various paths possible at a vertex and in general one must allow the possibility that the large  $\pm$  momentum will fragment and flow out the various arms of the vertex. Let us briefly consider the simplest such theory, having interaction  $H_I = \frac{1}{6} \lambda \varphi^3$ . This is particularly simple since we have already performed most of the integrals involved. For simplicity we put two

external legs of the vertex ( $\Gamma_{\varphi^3}$ ) on shell.

Let us compare everything to the bare vertex normalized to 1 as in QED. The  $O(\lambda^2)$  term comes from the diagram in Fig. 2(a). The only possible choice of pathways corresponds to the one we have already computed. From Eqs. (3.7) and (3.8) it is just

$$\Gamma_{\varphi^3}^{(1)} = \left( \frac{\lambda^2}{32\pi^2 Q^2} \right) \ln^2(Q^2/\mu^2). \quad (5.1)$$

Next consider  $O(\lambda^4)$ . The straight ladder diagram again has only one possible choice of pathways, so from Eq. (3.20) and the integration methods of Appendix A,

$$\Gamma_{\varphi^3(3a)} = \frac{1}{2} \times \frac{1}{3} \left( \frac{\lambda^2}{32\pi^2 Q^2} \right)^2 \ln^4(Q^2/\mu^2). \quad (5.2)$$

For the crossed double exchange, however, there are two choices of pathways. These are indicated by dot-dashed lines in Fig. 7. To find the asymptotic behavior it is sufficient to take the sum of the two choices computed separately; any partition of the large momentum between the two choices would have large  $+$  and  $-$  momentum flowing through a common line and hence would give an over-all contribution  $\sim Q^{-n}$ , where  $n > 4$ . By inspection, the two paths shown in Fig. 7 contribute identically.

Actually, as Eichten and Jackiw<sup>24</sup> have informed us, there are two additional paths which contribute to the asymptotic behavior of diagram 3(b). To find these additional paths let the large  $(+)$  momentum flow as drawn in one of the diagrams shown in Fig. 7 and the large  $(-)$  momentum flow as in the other. For these additional paths one internal line carries both large  $+$  and  $-$  momentum, and hence contributes  $\sim Q^{-2}$ , while two other internal lines carry only a single large  $\pm$  momentum. These paths therefore also contribute  $\sim Q^{-4}$ .

After having been informed of these additional paths, we have verified the result of Jackiw and Eichten that these paths contribute asymptotically  $\sim \ln^4 Q^2$  as do the paths indicated in Fig. 7. The total contribution of the four paths is

$$\Gamma_{\varphi^3(3b)} = \frac{1}{2} \times \frac{4}{3} \left( \frac{\lambda^2}{32\pi^2 Q^2} \right)^2 \ln^4(Q^2/\mu^2). \quad (5.3)$$

In writing Eq. (5.3) we have included the factor of  $\frac{1}{2}$  in the Feynman rules which arises from the fact that not all permutations of the internal vertices of Fig. 3(b) are topologically distinct. Note that the contribution of diagrams 3(a) and 3(b) is no longer the third term in an exponential series<sup>24</sup> in the variable  $\Gamma^{(2)} = (\lambda^2/32\pi^2 Q^2) \ln(Q^2/\mu^2)$ .

In sixth and in every order thereafter the scalar vertex ceases even to be a series in  $\Gamma^{(2)}$ . This is

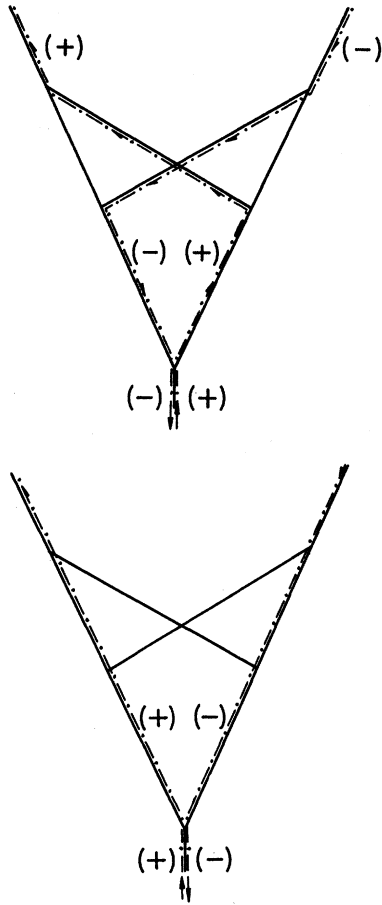


FIG. 7. Alternate paths for infinite momentum in a particular diagram. The (-) indicates large positive minus component is carried in the direction of the arrow; similarly the line with a (+) carries large plus component.

not because of incorrect numerical factors, but because of alternative pathways which lead to fewer powers of  $Q$  in the denominator. These paths are "shortcuts" which traverse fewer propagators than one might expect. An example in  $O(\lambda^6)$  is shown in Fig. 8. This path traverses four internal lines and gives, aside from logarithms, a contribution  $\sim Q^{-4}$  rather than the  $Q^{-6}$  which comes from the straight ladder in order  $\lambda^6$ . One also has trouble in scalar theories with self-energy and vertex insertions.<sup>6</sup> For example, the fourth-order diagram in Fig. 9 has an asymptotic behavior  $\sim Q^{-2} \ln^2 Q^2$  which overwhelms the  $Q^{-4} \ln^4 Q^2$  contribution of the straight ladder of the same order in  $\lambda$ . Problems such as these also occur in studies of the asymptotic form of the four-point function in scalar theories. Our remarks are not intended as a proof that the scalar vertex does not exponentiate. We merely wish to say that one cannot show it by summing the leading term in each order of perturbation theory; a complete reordering of

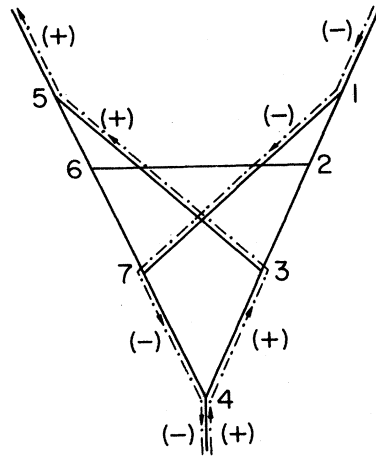


FIG. 8. A "shortcut" for infinite momentum which first arises in  $O(\lambda^6)$  is shown. It occurs in all higher orders as well.

the perturbation series would be necessary. For other than the self-energy and vertex insertions of, e.g., Fig. 9, such a reordering would plausibly take the following form.

We first redraw a particular pathway in a particular diagram with its large momentum flowing through the side legs of the diagram. The pathway of Fig. 8, for example, may be redrawn as in Fig. 10(a). We then suppose, as we shall discuss in Sec. VI, that the "exchange" of this unit when iterated and summed exponentiates by itself. [One possible iteration is shown in Fig. 10(b).] The argument of this exponential would be  $O(\lambda^6)$  contribution to  $\Phi$ . The sum of all iterations of the exchange of *both* a single particle and this new unit, with the infinite-momentum pathway restricted to the side legs, would exponentiate with an argument  $\Phi$  which is the sum of the  $\Phi$  for the separate exchanges. Such a new type of perturbation theory as a resolution to similar problems arising in the four-point function in scalar theory has been discussed previously.<sup>25</sup>

## VI. CONCLUSIONS

We have summed the leading behavior of a large class of diagrams in quantum electrodynamics (with massive photons) in order to find the behavior of the three-point function at large values of the momentum transfer  $Q^2$ . The class of diagrams we have studied form a gauge-invariant set and are those which involve no photon-photon scattering insertions (for vacuum polarization insertions see below). The leading diagrams for this class are those in which all internal photons are connected across the external photon vertex in all possible ways, i.e., all crossed- and uncrossed-ladder

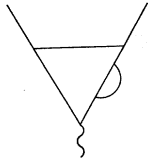


FIG. 9. A self-energy correction in  $\lambda\varphi^3$ . Infinite momentum through the two legs of the self-energy bubble must be partitioned in all possible ways.

(rainbow) diagrams.

We find that the vertex falls rapidly as  $Q^2 \rightarrow \infty$  in a particularly elegant form. The fall is faster than any fixed power of  $Q^2$ . More precisely,

$$\bar{u}(p_b)\Lambda^\mu u(p_a) = \bar{u}(p_b)\gamma^\mu u(p_a)e^{-\Phi}, \tag{6.1}$$

$$\Phi = \frac{e^2}{16\pi^2} \ln^2(Q^2/\mu^2).$$

This exponential form was conjectured by Jackiw<sup>7</sup> on the basis of his second- and fourth-order calculations. Since we have not kept next to leading terms, the scale factor  $\mu^2$  in Eq. (6.1) cannot be taken seriously. When the external fermions are off shell, we also find an exponential form which in the appropriate regime agrees with the calculations of Sudakov.<sup>8</sup> Although the above result was derived in the spacelike region  $Q^2 > 0$ , we believe that it holds everywhere. One merely replaces

$$\ln^2(-Q^2) \rightarrow (\ln|Q^2| - i\pi)^2 \cong \ln^2|Q^2| - i\pi \ln|Q^2|.$$

Physically, the damping of the elastic form factor – an exclusive quantity – reflects the unlikelihood of reabsorbing the bremsstrahlung, which can be emitted by the fermion when it suffers a large momentum transfer. The more likely processes are the inclusive ones – those allowing unrestricted emission of bremsstrahlung. The interplay between the two types of processes has been studied in detail for the scattering amplitude in scalar field theory.<sup>3</sup> It will be interesting to see how this goes for the vertex also. It is interesting to note also that a model by Mack<sup>26</sup> which embodies these physical ideas, but which assumes Poisson distributions for soft particle emission rather than

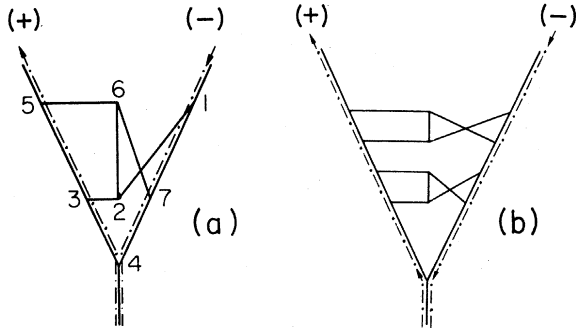


FIG. 10. (a) The diagram of Fig. 8 redrawn so that infinite momentum flows through the “external” legs. (b) Ladder-type iteration of diagram (a).

employing field theory, obtains an exponential vertex with an argument  $\sim \ln^2 Q^2$  as we have found.

The usual remarks about summing selected parts of the perturbation series should be applied to our work. There is no proof that we have obtained the leading piece of the complete vertex by summing the leading piece in each order of the coupling constant expansion. It may be, for example, that the next to leading terms occur in such overwhelming numbers that their sum exceeds the leading term. The hope that this does not happen corresponds physically to some sort of random-phase approximation – the next-to-leading terms do not add coherently. Mathematically what is required is proof of the uniform convergence of the perturbation series with respect to  $Q^2$ . Needless to say, we have not yet obtained this proof.

One interesting feature of our results is that the  $F_1$  form factor for spin- $\frac{1}{2}$  particles becomes identical as  $Q^2 \rightarrow \infty$  to the charge form factor of spin-0 particles (see Appendix B). This universality does not extend to all field theories, however. For  $\lambda\varphi^3$  theory, as  $Q^2 \rightarrow \infty$  only the bare vertex survives. More interestingly, as Appelquist and Primack<sup>5</sup> showed, the result is also different in neutral pseudoscalar pion-nuclear theory. In this latter theory the interesting diagrams in each order are the simple uncrossed-ladder (rainbow) diagrams. Crossed diagrams, corresponding to Fig. 3(b), are no longer leading. The vertex again exponentiates but with an exponent  $\sim \ln Q^2$  rather than the  $\ln^2 Q^2$  which we find. This change in the power of the logarithm occurs because the  $p$ -wave nature of the pion-nucleon coupling suppresses the infrared logarithm we obtained in the  $k^-$  integrations. When isospin is introduced into the pseudoscalar field theory or the vector-spinor theory, all simple results break down. One of the reasons for this is that the independence of events required for exponentiation – that photons must be emitted and absorbed in all possible positions on the fermion lines – breaks down in a theory with isospin. This is a problem which also plagues the eikonalization of the four-point function. It is also worth noting that radiative corrections on the sides are asymptotically important in the pseudoscalar theory, and also lead to a breakdown of the simple results.

One might imagine introducing a transverse momentum cutoff on phenomenological grounds as in Drell, Levy, and Yan.<sup>1</sup> While there is no unique way to introduce such cutoffs, the most reasonable way would simply modify the exponential argument of our vertex according to [see Eq. (3.7) or Appendix A]

$$\Phi \rightarrow \left( \frac{e^2}{16\pi^2} \right) \ln(Q^2/\mu^2) \ln(\Lambda^2/\mu^2),$$

where  $\Lambda \sim 300$  MeV is the transverse cutoff. This would change the asymptotic falloff to a power type with exponent depending on the coupling constant as well as the cutoff. Returning again to unsullied field theory, we saw that the quantity  $\Phi$  is modified by vacuum polarization insertions, e.g., Fig. 3(e).

The fact that the sum of all crossed- and uncrossed-ladder graphs has a much simpler form than any of the graphs separately is reminiscent of the field-theory calculations of scattering amplitudes which have been recently made.<sup>1</sup> There are important differences, however. In the scattering case the combination of the crossed and uncrossed diagrams resulted in the complete cancellation of the leading logarithmic terms. The total amplitude, then free of logarithms, was of a factorized form in an impact-parameter space. For the vertex case we study, there is no cancellation of the leading asymptotic terms of the separate diagrams. The simplification comes only in the coefficient of the asymptotic  $\ln^{2n} Q^2$  and leads to factorization of the vertex itself. One curious fact is that the contributions of the crossed- and uncrossed-ladder diagrams are identical in the far-off-shell Sudakov case but are unequal in the on-shell case. The greater the number of crosses, the greater is the coefficient of  $\ln^{2n} Q^2$ . (This is not obvious in the method presented in Secs. III and IV. It is clear already in Ref. 7 and can be seen in general by tedious applications of the integration procedure outlined in Appendix A.)

One might think that the asymptotic form of the vertex could be derived trivially by taking the known eikonal form for the scattering amplitude and closing one end by a single loop integration. The resultant expression is divergent, however, reflecting the fact that certain approximations valid for the on-shell scattering amplitude cannot be made for the off-shell amplitude which actually occurs in the vertex expression. Presumably what is required is an eikonal form for the off-shell scattering amplitude. Indeed progress along such lines for scalar field theories have been given recently by Cardy.<sup>27</sup>

Despite the differences between the vertex and scattering amplitude we conjecture that the exponentiation we have obtained for single-particle exchange (including vacuum polarization) generalizes to the exchange of more complicated structures; see the discussion in Sec. V. The argument  $\Phi$  of the exponential would then become the sum of the individual  $\Phi$ 's corresponding to the exchange of all possible connected units. We hope to report on this and other related matters at a later time.

#### ACKNOWLEDGMENTS

The authors wish to thank Shau-Jin Chang for

informative conversations. Upon completion of this manuscript we have learned that some of our results have been obtained independently using alternate methods by Appelquist and Primack. These authors have informed us that details of some of their work can be found in Ref. 28.

#### APPENDIX A

In this appendix we study the asymptotic behavior of the quantity defined by Eq. (3.7):

$$\Gamma^{(1)} = \frac{+e^2}{16\pi^2 Q^2} \int_0^\infty dx \int_{-\epsilon Q}^0 dk^- \left(k^- - \frac{b}{Q}\right)^{-1} \left(\frac{k^- a}{Q} - \Delta\right)^{-1}. \quad (\text{A1})$$

In going from Eq. (3.7) to Eq. (A1), we have carried out the trivial angular integration and introduced  $x = \vec{k}^2$ . Carrying out the  $k^-$  integration, one finds

$$\Gamma^{(1)} = + \frac{e^2}{16\pi^2 Q^2} \int_0^\infty \frac{dx}{(\Delta - ab/Q^2)} \times \left[ \ln(Q^2 \Delta / ab) - \ln\left(\frac{\epsilon}{\epsilon + \Delta/a}\right) + O(1/Q^2) \right]. \quad (\text{A2})$$

The leading  $\ln^2 Q^2$  behavior comes entirely from the first term in the square brackets; we drop the remaining terms. The important regions in the final  $x$  integration depend on the fermion masses  $m_a^2$  and  $m_b^2$ .

We take up first the on-shell case  $m_a^2 = m_b^2 = m^2$ . Then  $a = b = x$ , and  $\Delta - Q^{-2}ab = x + \mu^2 - Q^{-2}x^2$ . Only in the region where this denominator factor is varying  $\sim x$  can the integration build up a  $\ln^2 Q^2$ . This occurs for  $\mu^2 < x < Q^2$ ; more precisely for  $(1/\xi)\mu^2 \leq x \leq \xi'Q^2$ ;  $\xi, \xi' \ll 1$ . Thus

$$\Gamma^{(1)} \cong \left(\frac{e^2}{16\pi^2 Q^2}\right) \int_{+\mu^2/\xi}^{\xi'Q^2} \frac{dx}{x} \ln(Q^2/x) = \left(\frac{e^2}{16\pi^2}\right) \frac{1}{2Q^2} \ln^2(Q^2/\mu^2) + O((1/Q^2)\ln Q^2). \quad (\text{A3})$$

The off-shell case is similar but slightly more complicated. The final integration in Eq. (A2) can be done in closed form in terms of a Spence (dilogarithm) function, but the result is not particularly enlightening. Introduce the parameter  $\lambda = (m_a^2 - m^2)(m_b^2 - m^2)/(Q^2 \mu^2)$ . The important regions of integration in Eq. (A2) (we arbitrarily assume  $|m_a^2| < |m_b^2|$ ) for  $|\lambda| \gg Q^2 \gg |m_a^2|, |m_b^2| \gg m^2, \mu^2$  are

$$|\lambda| \mu^2 / \epsilon < x < \epsilon |m_a^2| \quad \text{and} \quad |m_b^2| / \epsilon < x < \epsilon Q^2.$$

In this region only, the integrand has an  $x^{-1}\ln x$  behavior which integrates to

$$\Gamma^{(1)}(Q^2, m_b^2, m_a^2) = \left(\frac{e^2}{8\pi^2}\right) \frac{1}{2Q^2} \left[ \ln\left(\frac{Q^2}{|m_a^2|}\right) \ln\left(\frac{Q^2}{|m_b^2|}\right) + O(\ln Q^2) \right], \quad (\text{A4})$$

as previously described by Sudakov.<sup>8</sup> Note that this result embodies scaling – the right-hand side is a function only of the two ratios of the three independent scalar variables.

The asymptotic form of  $\Gamma^{(1)}$  for other regions of  $\lambda$  which may be of interest is easily found by similar arguments. The quantity  $\lambda$  does not appear explicitly in Ref. 8 since there the massless photon ( $\mu^2 = 0$ ) case is assumed *ab initio*.

#### APPENDIX B

In this appendix we briefly discuss the electrodynamics of a spin-zero boson. (The boson takes the place of the fermion.) For ladder graphs of the general type we have been discussing, such as Fig. 3, the denominators, corresponding to a simple scalar theory, are as before. The numerator of, for example, Fig. 3(a) in this theory is

$$N^\mu = (-1)^2 (2p_1 + k_2)^{\alpha_1} (2p_1 + k_2 + k_1)^{\alpha_2} \times (p_2 + p_1 + 2k_2 + 2k_1)^\mu (2p_2 + k_2 + k_1)^{\alpha_2} (2p_2 + k_2)^{\alpha_1}. \quad (\text{B1})$$

The  $k_i$  which appear in the numerators cause the same divergences as in fermion electrodynamics and are treated in the same fashion. We therefore ignore them compared to the large components  $Q$  of  $p_1$  and  $p_2$ . This constrains  $N^\mu$  to be

$$N^\mu = (-2Q^2)^2 (p_2 + p_1)^\mu. \quad (\text{B2})$$

Ignoring the  $k_i$  in the numerators compared to  $Q$  once again has constrained the infinite momentum not to flow in the photon lines, else the entire function contains uncompensated powers of  $Q$  in the denominator. This fact also tells us that this numerator is the same for all diagrams with  $n$  photons exchanged. The factor  $(-2Q^2)^2$  for two photons exchanged becomes  $(-2Q^2)^n$  for  $n$  photons exchanged.

The main vertex, labeled with  $\mu$ , is quite differ-

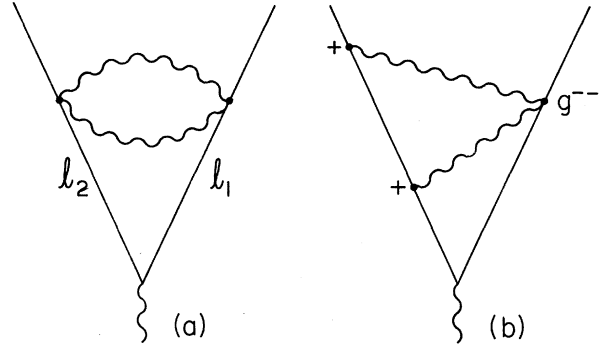


FIG. 11. Two examples of seagull diagrams which occur in scalar electrodynamics. Both are negligible asymptotically.

ent from fermion electrodynamics. In that case only  $\mu = \perp$  survives, with no extra momentum factors. In scalar electrodynamics both  $\mu = +$  and  $\mu = -$  survive, with large factor  $Q$ . In the more conventional four-momentum labeling, it is only the zero (or time) component which survives. This merely reflects the well-known fact that charged spin-0 fields contribute only to the scalar piece of the electromagnetic current. The coefficient of  $(p_1 + p_2)^\mu$ , the electromagnetic form factor, is the same falling exponential function that we found for fermion electrodynamics, Eq. (4.11).

In spin-0 electrodynamics there is one other class of diagrams we must study. These are the so-called seagull diagrams. In the fourth order, for example, these diagrams are illustrated in Fig. 11. Using these diagrams as examples, we shall show how all diagrams with quadratic vertices are asymptotically unimportant. Consider Fig. 11(a) first. The seagull coupling is just  $g^{\alpha_1 \alpha_2} g^{\alpha_1 \alpha_2} = 4$  with no momentum factors. Thus we cannot cancel the  $Q^{-2}$  factor coming from the propagators of the two internal boson lines  $l_1$  and  $l_2$ . In Fig. 11(b), the seagull vertex again fails to account for a factor  $Q$ . The left-hand photon vertices provide factors to cancel powers of  $Q$ , but in order to do this the coupling must be via the  $+$  component. Then  $g^{--} = 0$  appears at the seagull vertex. In order to achieve a nonzero factor at the seagull vertex, we are forced to give up a factor of  $Q$  in the left-hand side. Thus Fig. 11(b) is also  $O(Q^{-2})$  smaller than the diagrams 3(a) and 3(b).

\*Work supported in part by the National Science Foundation under Grant No. NSF GP 25303.

<sup>1</sup>As examples of the wide variety of citations available, we choose H. Cheng and T. T. Wu, Phys. Rev. D 1, 3414

(1970), and references cited therein; S. D. Drell, D. J. Levy, and T. M. Yan, Phys. Rev. 187, 2159 (1969); Phys. Rev. D 1, 1035 (1970); 1, 1617 (1970); S. J. Chang and P. M. Fishbane, *ibid.* 2, 1084 (1970); 2, 1104 (1970);

B. Hasslacher, D. K. Sinclair, G. M. Cicuta, and R. L. Sugar, *Phys. Rev. Letters* **25**, 1591 (1970).

<sup>2</sup>For a recent review of these matters see *Proceedings of the International Conference on Expectations for Particle Reactions at the New Accelerators, Madison, Wis., April, 1970* (Physics Department, University of Wisconsin, Madison, Wis., 1970).

<sup>3</sup>S. J. Chang and T. M. Yan, *Phys. Rev. Letters* **25**, 1586 (1970).

<sup>4</sup>S. Weinberg, *Phys. Rev.* **150**, 1313 (1966) and S. J. Chang and S. K. Ma, *ibid.* **180**, 1506 (1969).

<sup>5</sup>T. Appelquist and J. R. Primack, *Phys. Rev. D* **1**, 1144 (1970).

<sup>6</sup>M. Cassandro and M. Cini, *Nuovo Cimento* **34**, 1719 (1964).

<sup>7</sup>R. Jackiw, *Ann. Phys. (N.Y.)* **48**, 292 (1968).

<sup>8</sup>V. V. Sudakov, *Zh. Eksperim. i Teor. Fiz.* **30**, 87 (1956) [*Soviet Phys. JETP* **3**, 65 (1956)].

<sup>9</sup>See Eq. (2.6).

<sup>10</sup>We warn the reader that this usage is purely conventional.

<sup>11</sup>In what follows, when we cut off integrations we often replace these  $\lambda$  factors by unity. This is justified as follows: Since our integrals give logarithms and not powers, we find forms such as  $(\ln \lambda Q^2)^n = (\ln \lambda + \ln Q^2)^n \rightarrow \ln^n Q^2$  as  $Q^2 \rightarrow \infty$ .

<sup>12</sup>For the  $k^+$  integration this is not immediately obvious since we carried it out by contour integration. If we examine Eq. (3.5), however, we see that if  $|k^+| > \lambda Q$ , the integrand behaves like  $|k^+|^{-3}$ , while for  $|k^+| \ll \lambda Q$  it behaves like  $|k^+|^{-2}$ .

<sup>13</sup>For the off-shell case the spinors in Eq. (3.10) are understood to be suppressed.

<sup>14</sup>More precisely we are only interested in the proper vertex  $\Lambda_\mu(q^2, p^2, p^2)$ , to which diagrams 2(b) and 2(c) do

not belong.

<sup>15</sup>S. Weinberg, *Phys. Rev.* **118**, 838 (1960). See also J. D. Bjorken and S. D. Drell, *Relativistic Quantum Fields* (McGraw-Hill, New York, 1965).

<sup>16</sup>This of course is cancelled by the vertex renormalization in the well-known fashion.

<sup>17</sup>One can calculate this directly from the self-energy diagram using Cutkosky rules.

<sup>18</sup>Possible additional over-all factors of  $\ln k^2$  do not affect our argument.

<sup>19</sup>In writing these equations we have dropped the bare vertex terms on the left-hand side.

<sup>20</sup>Note that having made this approximation in Eq. (3.32), we learn the remarkable fact that the form factors  $\mathcal{F}_{1,10}$  which in general depend on both  $k^2$  and  $p^2$  are expressible in terms of  $p^2$  alone.

<sup>21</sup>See the technique discussed in Sec. III.

<sup>22</sup>Our discussion here is meant to apply to diagrams with no self-energy or vertex corrections. When such corrections are present the flow is more complex, as we discuss later on.

<sup>23</sup>G. Tiktopoulos, *Phys. Rev.* **131**, 480 (1963).

<sup>24</sup>E. Eichten and R. Jackiw, this issue, *Phys. Rev. D* **4**, 439 (1971).

<sup>25</sup>See, for example, S. J. Chang and P. M. Fishbane, *Phys. Rev. D* **3**, 1047 (1971), and S. J. Chang and T. M. Yan, Ref. 3.

<sup>26</sup>G. Mack, *Phys. Rev.* **154**, 1617 (1967).

<sup>27</sup>J. L. Cardy, University of Cambridge Report (unpublished). The generalized eikonal forms contained in R. Blankenbecler and R. Sugar, *Phys. Rev. D* **2**, 3024 (1970), also look inviting.

<sup>28</sup>J. R. Primack, Ph. D. thesis, Stanford University, 1970 (unpublished).